

# Development of the Cooling Technology on TRU Fuel Pin Bundle during Fuel Fabrication Process

## (3) Development of Analytical Tool

Takashi TAKATA<sup>1</sup> Akira YAMAGUCHI<sup>1</sup> Koichi HISHIDA<sup>2</sup> Taichiro KURODA<sup>2</sup>  
Kunihiro ITOH<sup>3</sup> Kazuo IKEDA<sup>3</sup>

<sup>1</sup> Osaka University, 2-1 Yamadaoka, Suita, Osaka, 565-0871 Japan

<sup>2</sup> Keio University, 3-14-1 Hiyoshi, Kohoku-ku, Yokohama, 223-8552 Japan

<sup>3</sup> Nuclear Development Corporation, 622-12, Funaiishikawa, Tokaimura, Ibaraki, 319-1111 Japan

Tel: +81-6-6789-7895, Fax: +81-6-6879-7889, Email: takata\_t@see.eng.osaka-u.ac.jp

**Abstract** – In the trans-uranium (TRU) fuel bundle fabrication process, a fuel pin is spirally-wrapped with a thin wire in order to keep a clearance between fuel pins and is laid horizontally. Air flows into the gaps vertically across the pin bundle so as to suppress temperature increase due to decay heat of TRU during the fabrication. From a safety point of view, an effective cooling is of importance. In the present study, an analytical tool, based on a subchannel thermal-hydraulics simulation, has been developed to investigate the thermal-hydraulic behavior and to predict the maximum temperature and the temperature distribution inside the fuel bundle.

### I. INTRODUCTION

In development of Fast Breeder Reactor (FBR) cycle in Japan, a low decontaminated fuel in which a trans-uranium (TRU) is included will be fabricated in a fuel factory. The TRU fuel has a heat generation due to decay heat. Hence an effective cooling system is required during the fabrication. For this purpose, the authors have the research project to establish the cooling technology<sup>1</sup>.

Figure 1 shows the schematic of the TRU fuel bundle and its cooling image during the fabrication process. A fuel pin is spirally-wrapped with a thin wire to keep a clearance between the fuel pins and is laid horizontally. Air flows into the clearance vertically across the fuel bundle.

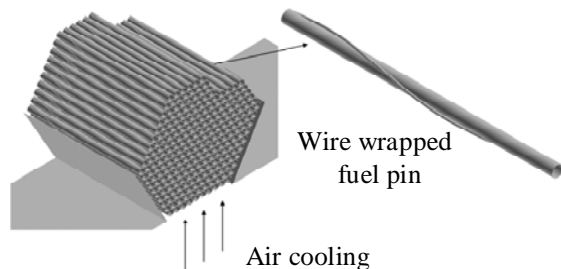


Fig. 1 Schematic of TRU fuel bundle and its cooling

It is also noted that the Fuel Assembly with Inner Duct Structure (FAIDUS)<sup>2</sup> is applied to the fuel pin bundle.

Therefore, a lack of fuel pins is seen in Fig. 1 (upper right side of the figure).

From the viewpoint of an engineering design development of the cooling system, it is preferable to develop an analytical simulation tool to predict the maximum temperature and the temperature distribution inside the bundle as well as the mocked up test results.

Consequently, an analytical tool specific to the TRU fuel has been developed in the present study based on a thermal-hydraulics simulation. Furthermore, a numerical experiment has also been carried out to extend the existing correlation, which is applied in the analytical tool, into the geometric configuration of the TRU fuel bundle using a multi-dimensional Computational Fluid Dynamics (CFD) tool.

### II. DEVELOPMENT OF ANALYTICAL TOOL

As a criterion of the engineering tool, the following terms are required in the present study.

- (1) Temperature distribution at each fuel pin and gap
- (2) Multi-dimensional effect caused by the wire.
- (3) Low computational cost

Since the TRU fuel bundle consists of more than 200 fuel pins, we select a subchannel analysis method taking the computational cost into account.

In a subchannel analysis method, a specific control volume inside a pin bundle is considered and the following governing equation in integral form is solved.

$$\begin{aligned} \frac{\partial}{\partial t} \langle \rho \phi \rangle + \frac{1}{\Delta V} \int_{Aff} \rho \phi \mathbf{u} \cdot \hat{\mathbf{n}} dA \\ = -\frac{1}{\Delta V} \int_{Aff} \mathbf{J} \cdot \hat{\mathbf{n}} dA - \frac{1}{\Delta V} \int_{Afs} \mathbf{J} \cdot \hat{\mathbf{n}} dA + \langle \rho S \rangle \end{aligned} \quad (1)$$

Here,  $\rho$  and  $\phi$  are the density and the unknown variable such as the velocity and the enthalpy.  $\mathbf{u}$  and  $\hat{\mathbf{n}}$  mean the velocity in vector form and the normal unit vector.  $\Delta V$ ,  $A$  and  $S$  are the volume, the surface area and the source and/or sink term respectively. The subscripts  $A_{ff}$  and  $A_{fs}$  represent the fluid-fluid and the fluid-solid interaction areas in the control volume.

In general, the subchannel analysis method is applied to a vertical allocated pin bundle. Besides, there is no boundary condition in the cross flow direction unlike the TRU bundle. Accordingly, an additional boundary condition is implemented in the present study as shown in Fig. 2.

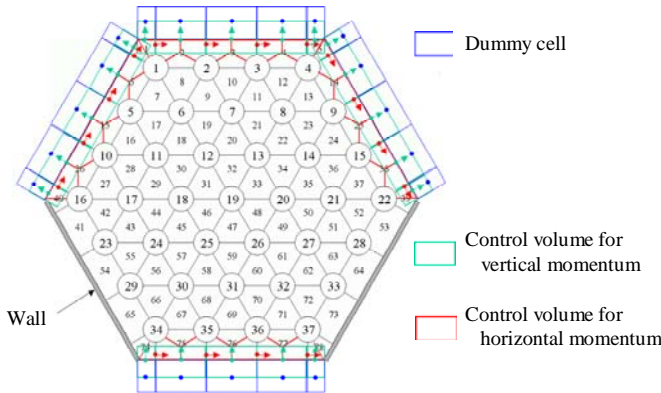


Fig. 2 Additional boundary conditions

The red and green boxed regions indicate the control volume for the horizontal and the vertical momentum conservations respectively. In order to enlarge the control volume of the vertical momentum conservation (green boxed region), dummy cells (blue boxed region) are embedded.

As the specific control volume is applied in the subchannel analysis method, constitutive correlations such as a flow resistance especially in the cross flow direction and a heat transfer coefficient will be of importance to ensure a predictive accuracy.

For instance, the Distributed Resistance Model (DRM)<sup>3</sup>, in which the flow resistance through the lateral and the axial directions of the pin and the wire can be evaluated separately, was established and was implemented into ASFRE-III code<sup>4</sup> to investigate the thermal-hydraulics behavior in a sodium-cooled fast reactor fuel bundle.

In the DRM model, an attached angle ( $\omega$ ) of the wire against the fuel pin affects the flow resistance in the lateral direction of the rod and in the normal direction of the wire as;

$$F_R^L \approx G(u) \frac{A_R}{A_w''} \quad (2)$$

$$F_w^N \approx G(v_n) \left( 1 - \frac{A_R}{A_w''} \right) \quad (3)$$

Here,  $F_R^L$  and  $F_w^N$  are the lateral component of force exerted by the fuel pin surface and the normal component of force exerted by the wire surface.  $A_R$  and  $A_w''$  are the fuel pin surface area and the total wetted surface including the wire.  $u$  and  $v_n$  are the lateral velocity component and the normal velocity component.  $G$  is introduced based on the correlations of such as Gunter-Shaw<sup>5</sup> and Zukauskas;

$$G(u) = \frac{A_w'' f_G}{8} \rho |u| u \left( \frac{D_V''}{S_T} \right)^{0.4} \left( \frac{S_L}{S_T} \right)^{0.8} \frac{1}{E(\omega)} \quad (4)$$

Where,  $f_G$ ,  $D_V''$ ,  $S_t$  and  $S_L$  mean the friction factor, without the wire (bare pin bundle), the equivalent hydraulic diameter including the wire surface, the fuel pin pitch and the distance between the fuel pins in a transverse row.  $E(\omega)$  indicates the influence of the attached angle of the wire and is defined in the following.

$$E(\omega) = \frac{f_G}{f_G^\omega} \quad (5)$$

Here,  $f_G^\omega$  is the friction factor in case of the wire-wrapped fuel pin bundle with attached angle  $\omega$ .

In the original model, the  $E$  function was determined based on the experiment<sup>7</sup>. However, the fuel pitch divided by the pin diameter (so called P/D) in the experiment (P/D=1.21) was larger than that in the present TRU fuel bundle configuration (P/D=1.10). Consequently, one has to confirm the capability of the existing  $E$  function or modify it to the TRU configuration. In the present paper, a numerical experiment has been carried out for this purpose.

### III. NUMERICAL EXPERIMENT OF E FUNCTION

In the numerical experiment, two dimensional benchmark analyses of the previous experiment<sup>7</sup> have been carried out firstly using the commercial CFD code FLUENT<sup>8</sup> Ver. 6.2 so as to investigate an applicability of the code to a pin bundle cross flow with wire. Then, the numerical examinations have been carried out by changing the P/D.

Figure 3 shows the analytical geometry that is same as the experiment. Each column consists of five pins and four rows are considered. A periodical boundary condition is applied both on the top and bottom side boundary (light blue color in Fig. 3).

An unstructured triangular cell (approximately 0.1mm on a side) is embedded so that an influence of nodalization diminishes and the total number of computational cell is approximately 420,000. It is noted that wire is not attached on some right edge pins both in the experiment and computation because of interference between the wire and the wall when it is attached at a low angle as shown in Fig. 3. A wide variety of the Reynolds number which is based on a hydraulic equivalent diameter and an average velocity at narrow gap was chosen in the experiment ( $Re = 10-12000$ ). In the analysis, the Reynolds number of 8000 is selected as an example.

In each computation, the pressure drop per row is evaluated and the friction factor is calculated. The turbulent model, such as the standard k- $\epsilon$ , the renormalization group (RNG) k- $\epsilon$  and the Reynolds stress model (RSM), and the Reynolds number ( $Re$ ), based on the hydraulic equivalent diameter and the average gap velocity, are chosen as an analytical parameter.

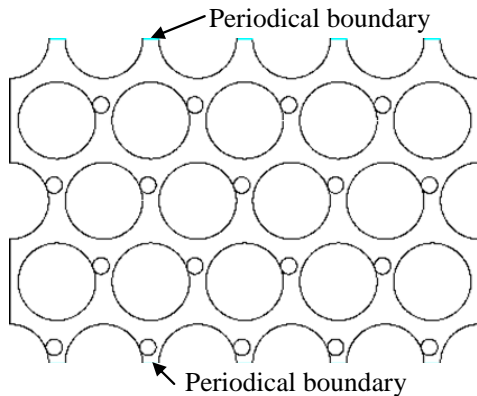


Fig. 3 Analytical geometry ( $\omega = 20^\circ$ )

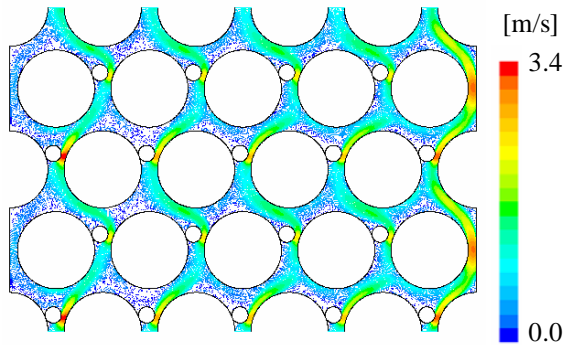


Fig.4 Velocity distribution (RNG k- $\epsilon$ ,  $Re \cong 8000$ ,  $\omega = 20^\circ$ )

Figure 4 shows the computational result of the velocity distribution (RNG k- $\epsilon$ ,  $Re \cong 8000$ ,  $\omega = 20^\circ$ ). The

main cross flow meanders through the wire. The comparison of the pressure drop per row is indicated in Fig. 5. The pressure drop changes in the range of 10-20% caused by a turbulent model. However, it agrees well with the experimental result in the range of the measurement uncertainty. With regard to the preferable turbulent model in the present study, we also have carried out the benchmark analysis of the enlarged partial model test<sup>9</sup>. As a result, the RNG k- $\epsilon$  model is selected.

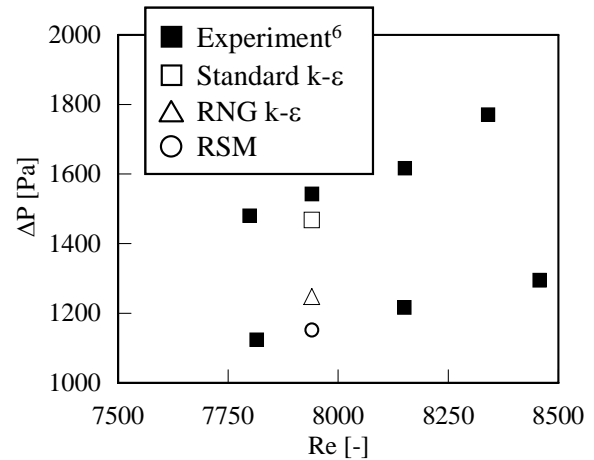


Fig. 5 Comparison of pressure drop per row ( $Re \cong 8000$ )

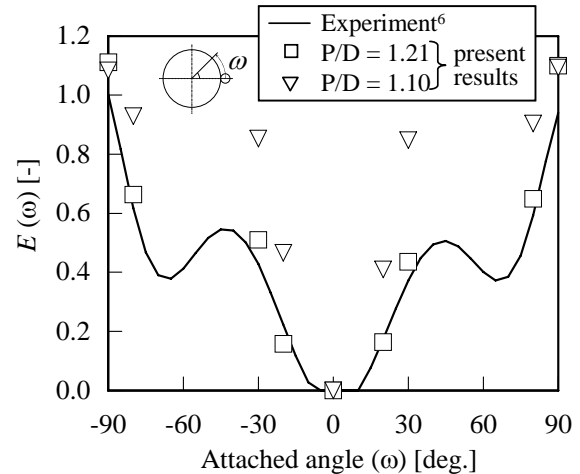


Fig. 6 Comparison of  $E$  function (RNG k- $\epsilon$ ,  $Re \cong 8000$ )

Figure 6 represents the  $E$  function both of the experimental and the numerical results. In the experiment, a fitted curve of eighth-order polynomial is established.

As seen in Fig. 6, it is again demonstrated that a good agreement is achieved in case of the same P/D (=1.21). The  $E$  function increases when the P/D becomes lower (=1.10). In case of lower P/D, the pressure drop due to contracted flow exerted by the narrow gap increases even in the bare pin bundle configuration. Consequently, the influence of the wire on the pressure drop decreases relatively resulting in the higher value of the  $E$  function.

It is noted that the value of the  $E$  function exceeds unit at  $\omega = \pm 90^\circ$  as in Fig. 6. This corresponds to the fact that the  $E$  function is evaluated using the Reynolds number based on the hydraulic equivalent diameter. Therefore, the mean velocity differs according to the attached wire.

In the numerical experiment of the  $E$  function, it is concluded that the commercial CFD code, FLUENT, is applicable to the  $E$  function evaluation and that the  $E$  function should be modified in accordance with the  $P/D$ .

#### IV. PRELIMINARY ANALYSIS WITH SUBCHANNEL TOOL

##### IV. A. Analytical Conditions

The preliminary benchmark analyses of the mocked up test<sup>1</sup> have been carried out using the developed subchannel tool. The geometry of the test apparatus is summarized in Fig. 7. The test bundle consists of 255 dummy fuel pin in which an electric rod type heater is installed to duplicate the decay heat. The uniform heating is added 1000mm in length as shown in Fig. 7.

The lower half and the both side ends of the bundle are covered with walls except the inlet opening at the bottom side. The opening is 1000mm×111mm wide which corresponds to the heating zone. A coolant gas (air) flows vertically into the test bundle through the opening.

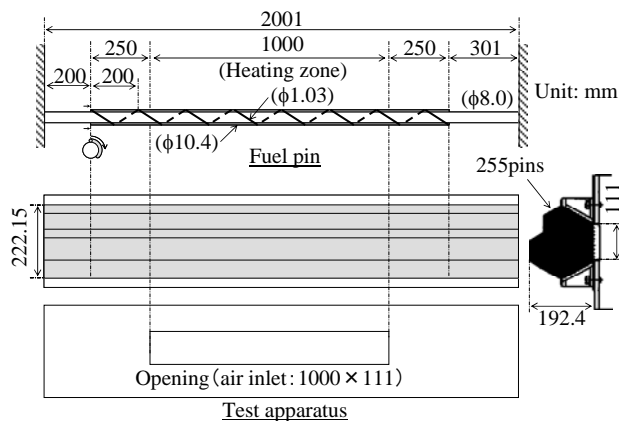


Fig. 7 Analytical geometry of mocked up test<sup>1</sup>

In the subchannel analysis, the axial direction of the test bundle is divided into 123 nodes and the wrapping wire is assumed to be laid horizontally at each node. In the heating zone, the axial mesh size is approximately 16.7mm that coincides with 1/12 of the wire wrapping pitch. The fuel pin tube (0.7mm in thickness) is also modeled.

As concerns a boundary condition, a constant heat flux is embedded on the inner surface of the fuel pin tube so that the total heat generation per fuel pin is equal to 5W. A uniform and constant inlet velocity of 1.0m/s (20°C) is assumed on the opening boundary. At the both ends of the fuel pin, a free-slip wall and an adiabatic condition is

applied. The maximum Reynolds number is approximately 2000 in the mocked up experiment.

Since the fuel pin is made in steel, conductivity inside the fuel pin tube will be of increasing significance in terms of the maximum temperature at the pin surface. Consequently, the manner of conductivity inside the fuel pin tube is treated as an analytical parameter in the present study. In Case1, the conductivity of radial direction is only taken into account. In addition, the conductivity of the circumferential direction is considered in Case2. The conductivity of all directions (radial, circumferential and axial) is assumed in Case3. It is noted that each outer fuel pin surface is coupled with 6 fluid cells in a subchannel analysis under a triangular pin arrangement. Hence, the same mesh dividing is applied to the circumferential direction of the fuel pin tube. The analytical condition is summarized in TABLE I.

TABLE I

Analytical condition of the mocked up test<sup>1</sup>

Number of fuel pin	255[-]
Heat generation	5W/pin
Inlet air velocity	1.0m/s
Atmospheric temperature	20°C
Conductivity inside pin tube	
Case1: 1 dimension (radial direction)	
Case2: 2 dimension (Case1 + circumferential direction)	
Case3: 3 dimension (Case2 + axial direction)	

##### IV. B. Results and Discussion

Figure 8 shows the temperature distributions of the outer surface of the pin bundle and the cross section along the axial direction. The cross sectional temperature and velocity distributions at the center of the heating zone is pictured in Fig. 9. The maximum temperature of the pin surface and the coolant gas at each case is summarized in TABLE II.

TABLE II

Maximum temperature of pin surface and coolant gas

Case No.	Pin surface	Coolant gas
1	104.5°C	102.0°C
2	93.9°C	91.1°C
3	74.1°C	72.0°C

As seen in Fig. 8, no axisymmetric temperature distribution is investigated at each case because the wire is wrapped spirally. The local maximum peak appears near the both ends of the heating zone.

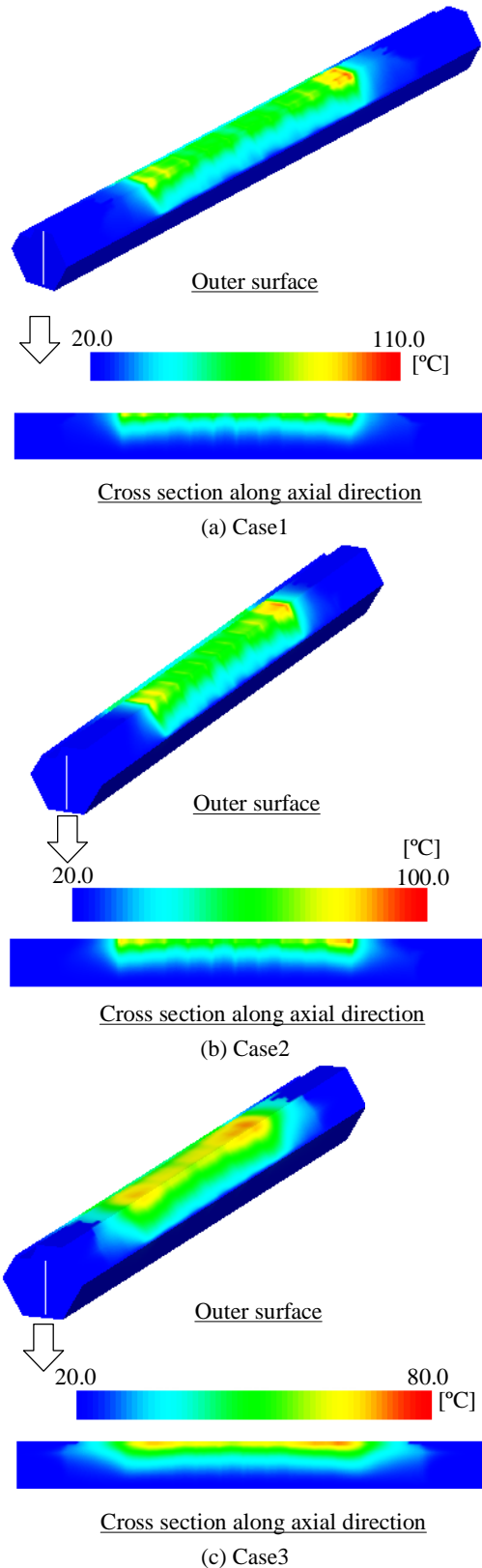


Fig. 8 Temperature distribution on outer surface and cross section along axial direction

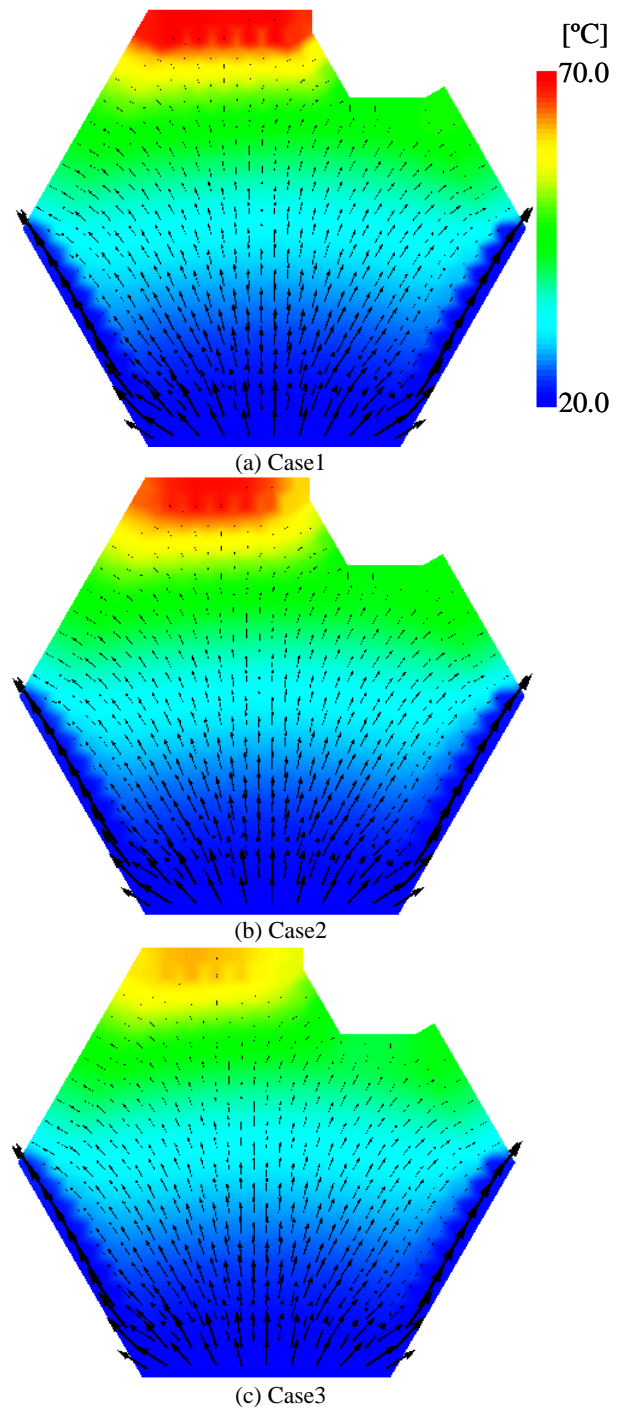


Fig.9 Velocity and temperature distribution at the center

This might be attributed the fact that the coolant gas flows away to the non heating zone at that region. Hence, a lower capability of heat removal due to convection is achieved comparing that at the center of the heating zone.

With regard to the velocity distribution shown in Fig. 9, large part of the coolant flows through the gaps between the wall and the fuel pin. Furthermore, the coolant flows away through the side openings at the upper half of the

bundle resulting in more decrease of the mass flow as it goes upward.

Consequently, a high temperature region appears at the top of the bundle as shown in Fig. 9. The gap between the side wall and the fuel pins is required to insert the pin bundle into a cover (wrapper) tube. Hence a new design which enhances the flow resistance at that gap is desirable during a building-up process of each fuel pin.

As shown in Figs. 8 and 9 and TABLE II, the conductivity in the circumferential and the axial directions inside the fuel pin tube affects the maximum temperature considerably. The maximum temperature decreases approximately 30°C when the multi-dimensional effect is considered. In the TRU fuel bundle fabrication, the mass flow of the coolant is not so much because only the decay heat should be removed. Therefore, a heat transfer due to conduction of fuel pin tube will not be negligible comparing with the convective heat transfer.

In the present analyses, the influence of the axial conductivity is superior to the circumferential conductivity as in TABLE II. This is attributed the fact that a low temperature change is investigated in the circumferential direction at each pin because of the comparative low heat generation. On the other hand, a high temperature gradient is predicted at the interface zone between the heating and the non-heating region (see Fig. 8). Therefore, the heat transfer in the axial direction becomes more influential on the maximum temperature than the circumferential heat transfer.

## V. CONCLUSIONS

In the present paper, a subchannel analysis tool has been developed in order to investigate the thermal-hydraulics behavior such as a maximum temperature and its spatial distribution during the fabrication of the TRU fuel pin bundle. Since the fuel pin bundle is laid horizontally during the fabrication, we have implemented the additional boundary condition in the cross flow direction which is specific to the TRU geometric configuration.

In the development of the subchannel analysis tool, the modification of the  $E$  function, which represents the influence of the wrapping wire on the flow resistance inside the pin bundle and is implemented into the Distributed Resistance Model (DRM), has also been carried out with the numerical experiment using the commercial CFD code, FLUENT.

As a result of the numerical experiment, it is concluded that the  $E$  function can be evaluated using the two-dimensional numerical simulation and that the  $E$  function will increase as the P/D (= pin pitch / pin diameter) decreases. This corresponds to the fact that the flow resistance due to contracted flow will increase more

when the P/D becomes lower. Hence, the influence of the wire will weaken.

Using the developed subchannel tool, the preliminary benchmark analyses of the mocked up test have been also carried out. In the analyses, the manner of the conductivity inside the fuel pin tube is chosen as a parameter. In each computation, non-axisymmetric temperature distribution is investigated and the local maximum peak appears near the both ends of the heating zone. It is also confirmed that the multi-dimensional effect of the fuel pin tube conductivity should not be negligible in the present study.

In the next stage of the subchannel tool development, the benchmark analyses of the mocked up test will be carried out to ensure a predictive accuracy of the tool. It is also intended that another numerical experiments of the constitutive model such as a heat transfer correlation will be carried out to enhance the predictive accuracy.

Furthermore, the code development for a transient state analysis where a termination of cooling system is assumed is also be planned in order to investigate a structural safety of the TRU fuel pin bundle during an incident.

## ACKNOWLEDGMENTS

Present study is the result of "Development of the Cooling Technology on TRU Fuel Pin Bundle during Fuel Fabrication Process" entrusted to "Nuclear Development Corporation" by the Ministry of Education, Culture, Sports, Science and Technology of Japan (MEXT).

## NOMENCLATURE

$A$	surface area in the control volume
$A_R$	fuel pin surface
$A_w^*$	total wetted surface including the wire
$D_v^*$	equivalent hydraulic diameter including wire surface
$F_R^L$	lateral component of force exerted by fuel pin
$F_w^N$	normal component of force exerted by wire
$f_G$	friction factor without wire (bare fuel pin bundle)
$Re$	Reynolds number based on hydraulic equivalent diameter and average gap velocity
$S$	source and/or sink per unit volume
$S_t$	fuel pin pitch
$S_L$	distance between fuel pins in a transverse row
$\hat{n}$	normal unit vector
$\mathbf{u}$	velocity in vector form
$u$	lateral velocity component
$v_n$	normal velocity component
$\Delta V$	volume

$\phi$  unknown variable  
 $\rho$  density

[Subscripts]

$A_{ff}$  fluid-fluid interaction area  
 $A_{fs}$  fluid-solid interaction area

#### REFERENCES

1. K. Itoh, et. al., "Development of the Cooling Technology on TRU Fuel Pin Bundle during Fuel Fabrication Process (1) Whole Study Plan and Fabrication of Test Apparatus", Proc. of ICAPP2008, **8306**, Anaheim, CA, USA, 2008
2. T. Mizuno and H. Niwa, "Advanced MOX Core Design Study of Sodium-cooled Reactor in Current Feasibility Study on Commercialized Fast Reactor Cycle System in Japan", J. of Nuclear Tech., **46, 5**, 2004
3. H. Ninokata, et. al., "Distributed Resistance Modeling of Wire-Wrapped Rod Bundles", J. of Nucl. Eng. and Design, **104, 93-102**, 1987
4. H. Ninokata, et. al., "ASFRE-III: A Computer Program for Triangular Rod Array Thermohydraulic Analysis of Fast Breeder Reactors", PNC, PNC N941 85-106, 1985
5. A. Y. Gunter and W. A. Shaw, "A General Correlation of Friction Factors of Various Types of Surfaces in Crossflow", Trans. Am. Soc. Mech. Eng., **57, 643-660**, 1945
6. A. Zukauskas and J. Ziugzda, "Heat Transfer of a Cylinder in Crossflow", Hemisphere Publishing Corp., 1985
7. K. Y. Suh and N. E. Todreas, "An Experimental Correlation of Crossflow Pressure Drop for Triangular Array Wire-Wrapped Rod Assemblies", Nucl. Tech. **76, 229-240**, 1987
8. <http://www.fluent.com>
9. K. Hishida, et. al., "Development of the Cooling Technology on TRU Fuel Pin Bundle during Fuel Fabrication Process (2) High-Speed PIV Measurement in Gap among Fuel Pin", Proc. of ICAPP2008, **8310**, Anaheim, CA, USA, 2008